Int J Thermophys (2009) 30:1960–1974
DOI 10.1007/s10765-009-0675-2

Investigation on Phase Transitions and Thermodynamic Properties of 1-Dodecylamine Hydrochloride ($C_{12}H_{25}NH_3Cl$)(s) by an Improved Adiabatic Calorimeter

Yu-Xia Kong · You-Ying Di · Ya-Qian Zhang · Wei-Wei Yang · Zhi-Cheng Tan

Received: 27 April 2009 / Accepted: 28 October 2009 / Published online: 13 November 2009

Abstract 1-Dodecylamine hydrochloride was synthesized by the solvent-thermal method. The structure and composition of the compound were characterized by chemical and elemental analyses, the X-ray powder diffraction technique, and X-ray crystallography. The main structure and performance of an improved automated adiabatic calorimeter are described. Low-temperature heat capacities of the title compound are measured by the new adiabatic calorimeter over the temperature range from 78 K to 397 K. Two solid-to-solid phase transitions have been observed at the peak temperatures of (330.78 ± 0.43) K and (345.09 ± 0.16) K. The molar enthalpies of the two phase transitions of the substance were determined to be $(25.718 \pm 0.082)\,\mathrm{kJ \cdot mol^{-1}}$ and $(5.049 \pm 0.055)\,\mathrm{kJ \cdot mol^{-1}}$, and their corresponding molar entropies were calculated as $(77.752 \pm 0.250)\,\mathrm{J \cdot mol^{-1} \cdot K^{-1}}$ and $(14.632 \pm 0.159)\,\mathrm{J \cdot mol^{-1} \cdot K^{-1}}$, respectively, based on the analysis of heat–capacity curves. Experimental values of heat capacities for the title compound have been fitted to two polynomial equations. In addition, two solid-to-solid phase transitions and a melting process of $C_{12}H_{25}NH_3Cl$(s) have been verified by differential scanning calorimetry.

Keywords Adiabatic calorimetry · 1-Dodecylamine hydrochloride · Low-temperature heat capacity · Phase transitions

Y.-X. Kong · Y.-Y. Di (✉) · Y.-Q. Zhang · W.-W. Yang
College of Chemistry and Chemical Engineering, Liaocheng University, Liaocheng 252059, Shandong Province, People's Republic of China
e-mail: diyouying@126.com; yydi@lcu.edu.cn

Z.-C. Tan
Thermochemistry Laboratory, Dalian Institute of Chemical Physics, Chinese Academy of Sciences, Dalian 116023, People's Republic of China

1 Introduction

Research on solid-state phase-change materials used for thermal energy storage has been studied for many years and received much attention by researchers. High energy density, a simple device, small size, and flexible design are the advantages of this kind of material, and they are also user-friendly and easy to handle. Therefore, investigations on a solid-state phase change in all kinds of energy storage materials are most frequently conducted as a result of the wide applications of these materials. The *bis*(*n*-alkylammonium) halometallates(II) (abbreviated as $C_{12}M$) [1–4] are important organometallic compounds of the general formula $(C_{12}H_{25}NH_3)_2MX_n$ ($n = 4$ or 6), where M is a divalent or trivalent metal ion and X is a negative haloid ion. They are characterized by a high enthalpy change and excellent reversibility of a solid-to-solid phase transition between two polymorphic forms in the temperature range 273 K to 393 K. As the necessary intermediate or raw material, 1-dodecylamine hydrochloride ($C_{12}H_{25}NH_3Cl$) plays an important role in the formation of $C_{12}M$ in which the $C_{12}H_{25}NH_3^+$ cation bonds with the MX_n^{2-} anion through ionic bonds.

1-Dodecylamine hydrochloride is important for agricultural applications as one of the important organic components of emulsifiers and insecticides. In medicine, it has a specific function in the treatment of skin burn as an antimicrobial. Also, it is a raw material of detergents in the fine chemical industry.

Adiabatic calorimetry is the most reliable method to obtain heat capacities and various thermodynamic data of substances. It is an important and effective experimental method used for the study of solid-to-solid phase transitions by measuring low-temperature heat capacities and calculating relevant thermodynamic properties. Heat capacity is one of the most fundamental thermodynamic properties of materials and necessary for many theoretical studies in physics, chemistry, and engineering technology which are related to materials. Much work has been done to measure heat capacities with adiabatic calorimetric instruments all over the world [5–11]. Traditional adiabatic calorimetric experiments have the disadvantages of complicated experimental procedures and large amounts of data to be treated for the purpose of high precision heat-capacity data. Compared with traditional devices, the experimental operation procedures for the newly improved adiabatic calorimeter have been greatly simplified by using modern computer technology and control theory on the basis of our previous automated adiabatic calorimeter. It has the advantages of a compact data acquisition and process system, advanced intellectual level, powerful processing ability of the software, better stability of measurement, and higher reliability of data acquisition.

In this study, low-temperature heat capacities and thermodynamic properties of the title compound were determined by a precision automated adiabatic calorimeter over the temperature range from 78 K to 397 K. Two solid-to-solid phase transitions of the title compound have been investigated by means of the analysis of the heat–capacity curve. The two solid-to-solid phase transitions and the melting process were further studied by the differential scanning calorimetry (DSC) technique.

2 Experimental

2.1 Synthesis and Characterization of 1-Dodecylamine Hydrochloride ($C_{12}H_{25}NH_3Cl$(s))

1-Dodecylamine and hydrochloric acid (37 mass%) chosen as the reactants and anhydrous alcohol (A.R.) used as the solvent were of analytical grade. 1-Dodecylamine was dissolved into the targeted amount of the anhydrous alcohol in a three-neck flask, and an excessive amount of hydrochloric acid (37 %) was gradually added to the above solution under sufficient stirring. The solution was boiled and refluxed for 2 h, where after the mixture was condensed by boiling off some of the liquid until a crystal membrane emerged from the solution surface. The final solution was cooled naturally to room temperature, filtered, and a white crystal was obtained. Then, the product was recrystallized thrice with anhydrous alcohol. White crystal was gained. Finally, the sample was placed in a vacuum desiccator at a temperature of 50 °C to dry for 6 h. The final product was inserted into a weighing bottle in a desiccator. The theoretical contents of Cl, C, H, and N in the compound have been calculated to be 15.98 mass%, 64.98 mass%, 12.72 mass%, and 6.32 mass%, respectively. Chemical and element analyses (Model PE-2400, Perkin-Elmer, Norwalk, CT, USA) have shown that the practical contents of Cl, C, H, and N in the compound have been measured to be 16.00 mass%, 64.96 mass%, 12.75 mass%, and 6.29 mass%, respectively. This showed that the purity of the sample prepared was higher than 0.9950 in mass fraction.

The X-ray powder diffraction (XRD) technique was used to determine whether the newly synthesized compound is novel or not. XRD spectra of 1-dodecylamine hydrochloride have been plotted in Fig. 1. The step length of the powder diffraction angle was 0.01°, the wave length was 0.154056 nm ($CuK_\alpha 1$ radiation), the electric voltage was 36 kV, and the electric current was 20 mA. The scanning rate was $4^\circ \cdot \mathrm{min}^{-1}$, and a graphite monochromator was used for the filtration. It was observed from Fig. 1 that there are several distinct characteristic absorption peaks that appeared in the angle range of $2\theta = 14°$, 19°, 20°, 22°, 24°, and 37° in the diffractogram of 1-dodecylamine hydrochloride.

Single crystals suitable for X-ray crystallography were mounted on a fiber. All diffraction data for the compound were collected on a Bruker Smart-1000 CCD area-detector diffractometer with graphite monochromated MoK_α radiation $(\lambda = 0.71073\ \text{Å})$ at 298(2) K using the program SMART and processed by SAINT-plus [12]. Absorption corrections were applied by SADABS. The structures was solved by direct methods and different Fourier synthesis using the SHELXTL-97 program, and refined with a full-matrix least-squares technique on F^2. All non-hydrogen atoms were refined anisotropically. All H-atoms were located theoretically and refined. The structural plots were drawn using SHELXTL and OLEX programs.

2.2 Adiabatic Calorimetry

An improved precision automated adiabatic calorimeter was used to measure the heat capacities of the compound over the temperature range $78 \leq (T/\mathrm{K}) \leq 400$. The

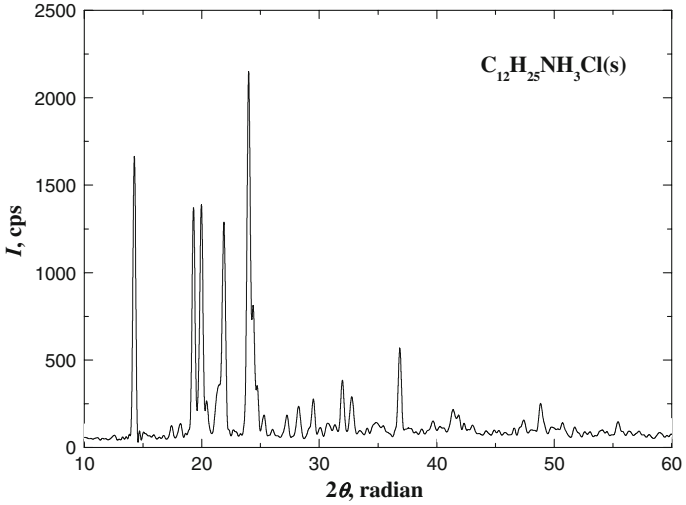

Fig. 1 XRD spectrum of 1-dodecylamine hydrochloride

calorimeter was established in the Thermochemistry Laboratory, College of Chemistry and Chemical Engineering, Liaocheng University, China. The principle and structure of the adiabatic calorimeter were described in detail elsewhere [13,14].

The new calorimetric system included a calorimetric cryostat, a data collection system, an adiabatic control system, and a high vacuum pump system. The calorimetric cryostat was composed mainly of a sample cell, a platinum resistance thermometer, an electric heater, inner, middle, and outer adiabatic shields, and three sets of six-junction chromel-copel thermocouple piles installed between the calorimetric cell and the inner shield, between the inner and middle shields, and between the middle and outer shields. The miniature platinum resistance thermometer (IPRT No. 2, Shanghai Institute of Industrial Automatic Meters, 16 mm in length, 1.6 mm in diameter, and a nominal resistance of 100 Ω) was used to measure the temperature of the sample. The thermometer was calibrated on the basis of ITS-90 by the Station of Low-Temperature Metrology and Measurements, Academia Sinica. A schematic diagram of the adiabatic calorimetric system is shown in Fig. 2.

The data collection system consisted of a multi-channel data acquisition/switch unit (Agilent 34970A) for electric energy collection, a 7 1/2 digit nanovolt/micro-ohm meter (Agilent, 34420A) for determination of the temperature of the sample cell, and a P4 computer equipped with a matched module and GPIB interface card (IEEE 488). The adiabatic control system consisted of a high precision temperature controller (Model 340, Lake Shore), inner, middle, and outer adiabatic shields, and three sets of six-junction chromel-copel thermocouple piles.

The sample cell (Fig. 3) used for the heat–capacity measurements was made of 0.3 mm thick gold-plated copper, 20 mm in length, and 20 mm in diameter with an inner volume of about 6 cm^3. Three sheaths were fixed at the bottom of the cell for inserting the platinum resistance thermometer and thermocouples. Electric heating wire (insulated Karma wire of 0.12 mm in diameter, $R = 120\ \Omega$) was bifilarly wound

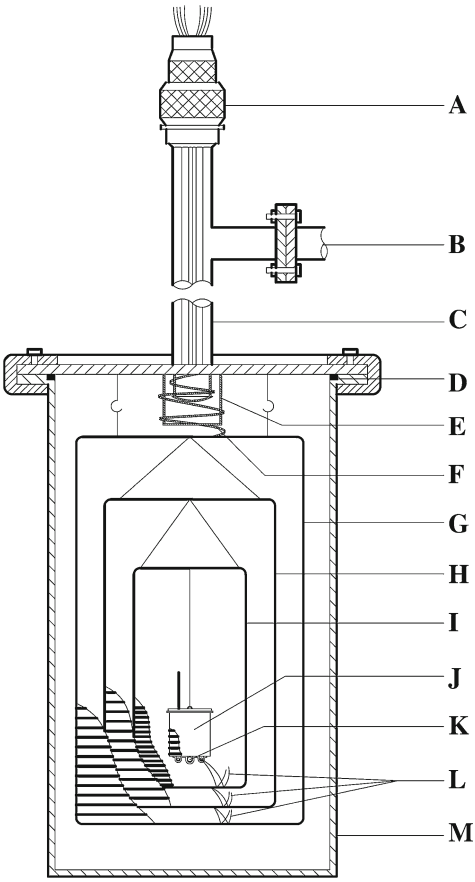

Fig. 2 Schematic diagram of the adiabatic calorimetric system: *A*, sealing junction unit; *B*, to high vacuum system; *C*, vacuum tube; *D*, fuse gasket; *E*, temperature controlled ring; *F*, lead wire bundles; *G*, outer adiabatic shield; *H*, middle adiabatic shield; *I*, inner adiabatic shield; *J*, sample cell; *K*, sheath for differential thermocouples; *L*, miniature platinum resistance thermometer; *M*, body of vacuum can

on the outer surface of the cell to serve as the heater of the cell. The heater was covered with about 50 μm thick aluminum foil to decrease the radiation heat leakage and the temperature graduation on the surface of the cell. The heater and aluminum foil were insulated and fixed by W30-11 varnish. A small amount of silicone thermally conducting sealant (Type HT916, produced by Shanghai Huitian New Chemical Material Company, Limited Shanghai, China) was used to seal the lid to the main body of the cell. On the lid, there was a section of copper capillary for pumping out the air in the cell and introducing the helium gas to promote thermal equilibrium. The capillary was pinched off and the resultant fracture was soldered to ensure the sealing of the cell.

To verify the accuracy of the calorimeter, heat capacities of synthetic sapphire (α-Al_2O_3), Standard Reference Material 720, were measured over the temperature range $78 \leq (T/\mathrm{K}) \leq 400$. The sample mass used was 1.7143 g, which was equivalent to 0.0168 mol based on its molar mass, $M(Al_2O_3) = 101.9613\,\mathrm{g \cdot mol^{-1}}$. In order to compare the values with those recommended by NIST [15], the molar heat capacities of α-Al_2O_3 in the temperature range of 80 K to 400 K were calculated at an interval of 5 K using the non-linear inserting method based on the measured molar

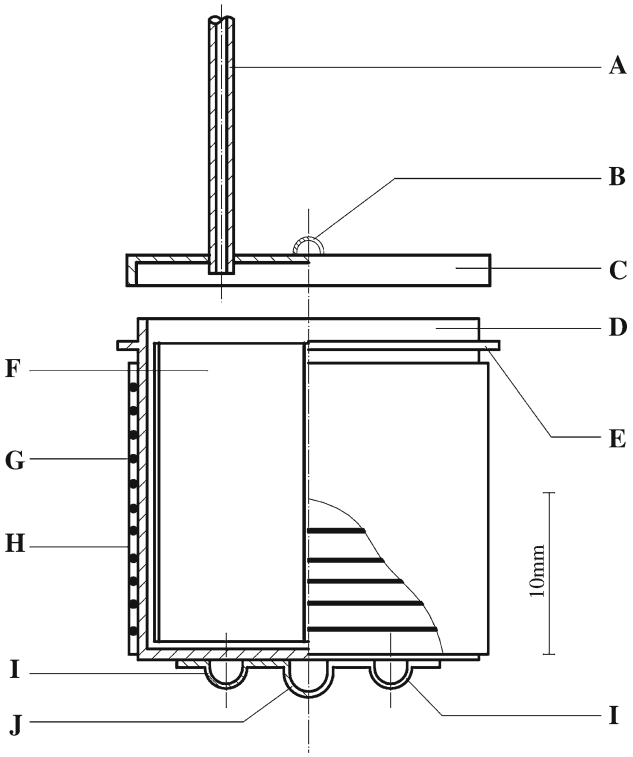

Fig. 3 Cross-sectional view of the calorimeter sample cell: *A*, copper capillary; *B*, lid ring; *C*, gold-plated copper lid; *D*, main body of the sample cell; *E*, sealing flange; *F*, gold-plated copper vane; *G*, Karma heating wire; *H*, aluminum foil; *I*, sheath for thermocouple; *J*, sheath for platinum thermometer

heat–capacity data. The temperature variability of the balance period is an important indicator used to weigh the stability and reliability of the adiabatic system in the experimental process. The variability of the temperature in the equilibrium period of all the measured points was within $-0.30\,\mathrm{mK}\cdot\mathrm{min}^{-1}$ to $+0.30\,\mathrm{mK}\cdot\mathrm{min}^{-1}$ in the temperature range of 78 K to 400 K. The heat capacity curve of synthetic sapphire (α-Al_2O_3) is shown in Fig. 4, and most of the deviations of our values from the recommended values [15] are within $\pm 0.30\,\%$, which demonstrates that the performance of the newly constructed calorimetric apparatus has been improved compared with previous calorimeters.

Heat–capacity measurements were continuously and automatically carried out by means of the standard method of intermittently heating the sample and alternately measuring the temperature. The heating rate and temperature increments were generally controlled at $0.1\,\mathrm{K}\cdot\mathrm{min}^{-1}$ to $0.4\,\mathrm{K}\cdot\mathrm{min}^{-1}$ and 1 K to 3 K. The heating duration was 10 min, and the temperature drift rates of the sample cell measured in an equilibrium period were always kept within $10^{-3}\,\mathrm{K}\cdot\mathrm{min}^{-1}$ to $10^{-4}\,\mathrm{K}\cdot\mathrm{min}^{-1}$ during the acquisition of all heat–capacity data. The data for the heat capacities and corresponding equilibrium temperatures have been corrected for heat exchange of

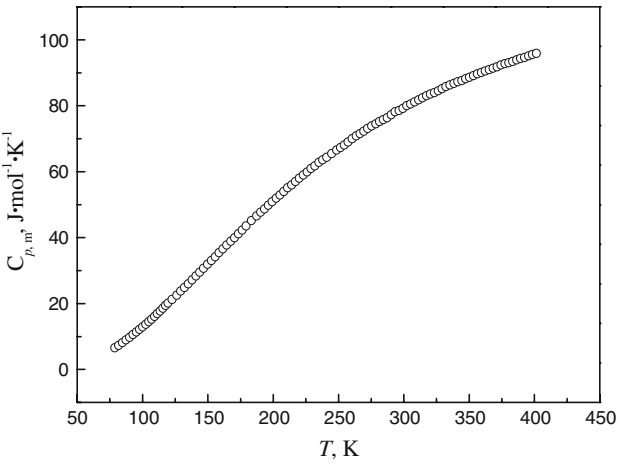

Fig. 4 Experimental molar heat capacities of α-Al_2O_3

the sample cell with its surroundings [13]. The sample mass used for calorimetric measurements was 1.8091 g, which was equivalent to 0.008156 mol in terms of its molar mass, $M = 221.81\,\mathrm{g \cdot mol^{-1}}$.

2.3 Differential Scanning Calorimetry

DSC analysis was carried out in a Perkin-Elmer diamond DSC. 1.86 mg of sample was weighed in a closed pan, placed in the DSC cell, and heated at the rate of $10\,\mathrm{K \cdot min^{-1}}$ in a flow of high-purity nitrogen.

3 Results and Discussion

3.1 Structural Description

The molecular structure of 1-dodecylamine hydrochloride ($C_{12}H_{25}NH_3Cl$) is shown in Fig. 5. The compound is monoclinic $P2_1/m$; unit cell dimensions are $a = 5.6680(8)$Å, $b = 7.1783(5)$Å, $c = 17.7385(18)$Å; $\beta = 92.7740(10)°$, and $Z = 2$. The geometries of the hydrogen bonding are listed in Table 1. Hydrogen bonds of N(1)–H(1A)···Cl(1), N(1)–H(1B)···Cl(1), and N(1)–H(1C)···Cl(1) together with the Van der Waals force exist in the crystal to stabilize the structure. These hydrogen bonds and intermolecular forces form a configuration with a two-dimensional layer that can be clearly identified in Fig. 6, in which the crystal structure was arranged along *ab* and *bc* axial planes. The results reveal that the hydrogen bonds play important roles in stabilizing the whole structure of the compound.

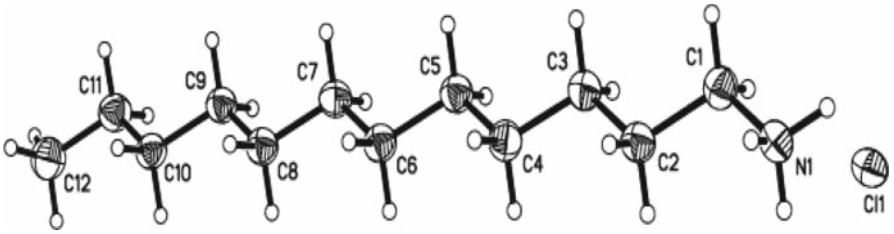

Fig. 5 Molecular structure of 1-dodecylamine hydrochloride

Table 1 Geometry of hydrogen bonds for $C_{12}H_{25}NH_3Cl(s)$

D–H···A	d(D–H)(Å)	d(H···A)(Å)	<DHA(°)	d(D···A)(Å)	Symmetry code
N(1)–H(1A)–Cl(1)	0.890	2.274	178.92	3.164	–
N(1)–H(1B)–Cl(1)	0.890	2.282	160.38	3.135	$[-x, -y+1, -z+1]$
N(1)–H(1C)–Cl(1)	0.927	2.291	152.42	3.142	$[-x+1, -y+1, -z+1]$

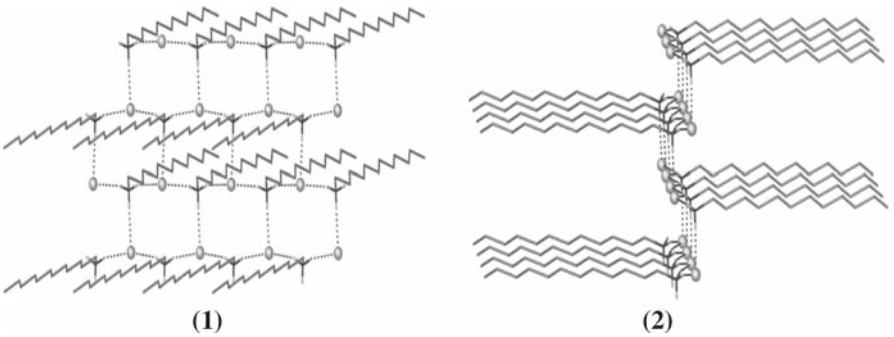

Fig. 6 Structure linked by hydrogen bonds along axial planes of *ab* (1) and *bc* (2)

3.2 Heat Capacity

All experimental results are listed in Table 2 and plotted in Fig. 7. It is shown that the structure of the compound is stable over the temperature range between 78 K and 326 K. However, there are two peaks that appear on the curve of experimental molar heat capacities over the temperature range from 326 K to 352 K.

The melting point of the title compound is measured to be about 181.5 °C to 183.0 °C (454.65 K to 456.15 K) according to the results obtained from the microscopic melting-point device. Therefore, two peaks appearing in the curve of experimental molar heat capacities were ascribed to solid-to-solid phase transitions. A reasonable explanation [16] may be that the first phase transition ($T_{trs,1}$) from the low-temperature phase ($P2_1/m$) to the intermediate-temperature phase is possibly due to the breaking of hydrogen bonds and leads to a dynamic order–disorder transition of rigid alkyl chains, whereas the second phase transition ($T_{trs,2}$) from the intermediate-to-high-temperature phase is related to cooperative conformational changes of the alkyl chains and assumes the complete disorder of the conformation similar to a "molten" state.

Table 2 Experimental molar heat capacities of $C_{12}H_{25}NH_3Cl(s)$ ($M = 221.81\,g \cdot mol^{-1}$)

T(K)	$C_{p,m}$ ($J \cdot mol^{-1} \cdot K^{-1}$)	T(K)	$C_{p,m}$ ($J \cdot mol^{-1} \cdot K^{-1}$)	T(K)	$C_{p,m}$ ($J \cdot mol^{-1} \cdot K^{-1}$)
78.701	127.14	173.96	229.12	293.88	353.17
80.270	130.02	176.88	231.57	296.86	357.94
82.622	133.30	179.86	234.47	299.88	361.61
84.975	136.93	183.94	238.61	302.82	366.09
87.290	139.87	188.17	241.94	305.84	369.94
89.500	143.35	191.00	244.85	308.78	374.86
91.670	146.02	193.98	247.44	311.76	380.61
93.758	149.07	196.96	250.16	314.74	386.41
95.797	151.77	199.94	253.12	317.75	393.33
97.992	154.07	202.92	256.21	320.75	400.56
99.875	156.32	205.90	258.25	323.72	409.86
101.91	158.73	208.88	260.60	326.65	428.81
103.80	160.53	211.83	263.92	329.38	586.05
105.83	162.77	214.84	266.83	330.78	3692.1
107.68	164.51	217.82	270.04	331.09	4112.9
109.56	166.22	220.80	272.58	331.52	5594.9
111.48	168.39	223.76	275.20	332.12	2469.3
113.21	171.31	226.71	278.00	334.31	1239.0
115.09	172.99	229.74	281.10	338.11	720.75
116.81	174.45	232.56	284.00	341.63	692.17
118.70	176.19	235.54	286.54	344.06	1344.8
120.42	177.86	238.68	289.93	347.28	626.02
123.09	180.51	242.60	293.94	351.29	517.24
126.54	184.46	246.36	297.30	354.42	500.39
129.52	187.56	249.29	300.24	357.40	500.74
132.50	190.61	252.27	302.72	360.54	501.04
135.48	193.71	255.24	306.26	363.52	501.38
138.30	196.80	258.19	310.06	366.50	501.78
141.32	199.50	261.13	313.41	369.64	502.22
144.26	202.54	264.05	316.42	372.62	502.64
147.24	204.88	267.03	319.75	375.75	502.99
150.22	207.85	270.07	322.89	378.73	503.40
153.20	210.44	273.02	326.44	381.71	503.77
156.18	212.67	276.00	330.08	384.85	504.21
159.16	216.06	279.14	333.91	387.83	504.63
162.14	218.35	282.03	337.69	390.81	505.00
165.12	221.38	284.94	341.76	393.95	505.42
167.94	223.78	287.92	345.77	396.93	505.82
170.92	226.32	290.90	349.66		

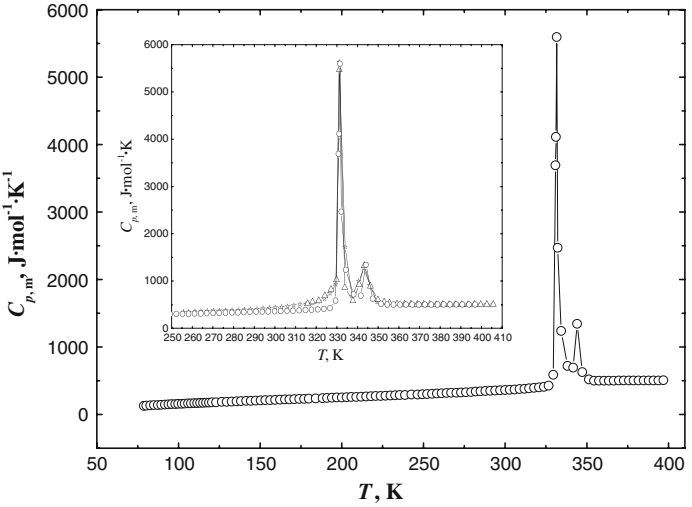

Fig. 7 Plot of heat capacities ($C_{p,\mathrm{m}}$) against temperature (T) of $C_{12}H_{25}NH_3Cl$(s): (◯) first series, (△) second series, and (☆) third series of heat–capacity measurements

In the intermediate phase, the rigid alkyl chains are flipping around their long axes between two equivalent orientations separated by 90°. The two transitions are somewhat analogous to the ones found in lipid bilayer membranes and can be described by order parameters used for smectic liquid crystals.

The 89 experimental points in the temperature region from 78 K to 326 K before the first phase transition, and the 15 experimental points between 352 K and 397 K after the second phase transition were fitted by means of least squares, and two polynomial equations of the experimental molar heat capacities ($C_{p,\mathrm{m}}/\mathrm{J}\cdot\mathrm{mol}^{-1}\cdot\mathrm{K}^{-1}$) versus reduced temperature (X), $X = f(T)$, have been obtained:

(1) Before the two phase transitions in the temperature range from 78 K to 326 K,

$$C_{p,\mathrm{m}}/(\mathrm{J}\cdot\mathrm{mol}^{-1}\cdot\mathrm{K}^{-1}) = 254.981 + 110.096X + 5.867X^2 + 29.826X^3 + 7.749X^4$$

where X is the reduced temperature, $X = (T - 202)/124$, in which 202 is half of the upper limit (326 K) plus the lower limit (78 K) in the temperature region of 78 K to 326 K, and 124 is half of the upper limit (326 K) minus the lower limit (78 K) in the same region. The reduced temperature (X) obtained by the method was located between +1 and −1, and deviations of the smoothed heat capacities from the experimental values would become smaller and smaller with an increase of the power of the fitted polynomial equation according to the statistical principle. The correlation coefficient for the fit was $R^2 = 0.9998$. The above equation is valid in the temperature range from 78 K to 326 K, with an uncertainty of 0.40 % except for several points around the lower and upper temperature limits.

(2) Above the two phase transitions in the temperature range from 352 K to 397 K,

$$C_{p,\mathrm{m}}/(\mathrm{J}\cdot\mathrm{K}^{-1}\cdot\mathrm{mol}^{-1}) = 502.842 + 2.996X + 0.019X^2 - 0.173X^3 + 0.150X^4$$

where $X = (T - 374.5)/22.5$. The correlation coefficient for the fit was $R^2 = 0.99982$. The above equation is useful in the temperature range from 352 K to 397 K, with an uncertainty of 0.25 %.

3.3 Molar Enthalpies and Entropies of Phase Transitions

Three series of the experiments in the two-phase transition region of the title compound with different cooling rates of the sample were carried out so that the reversibility and repeatability of the phase transition region of the sample were verified. The cooling rate of series 1 was about $15\,\mathrm{K}\cdot\mathrm{min}^{-1}$ (liquid nitrogen as the coolant), that of series 2 was about $2.5\,\mathrm{K}\cdot\mathrm{min}^{-1}$ (ice-water cooling), and that of series 3 was about $0.5\,\mathrm{K}\cdot\mathrm{min}^{-1}$ (natural cooling). The results of the three series of heat capacity measurements are reported in Table 3 and plotted in Fig. 7. It may be seen from Fig. 7 that there were some slight differences in heights and widths of peaks corresponding to each series of heat–capacity measurements during the phase changes. However, the two phase transitions basically exhibited good reversibility and repeatability. Different cooling rates did not affect the experimental results. Near agreement in $C_{p,\mathrm{m}}$ values of each series of repeated experiments was obtained. The molar enthalpies $\Delta_{\mathrm{trs}}H_{\mathrm{m}}(\mathrm{kJ}\cdot\mathrm{mol}^{-1})$ of two phase transitions were evaluated in terms of the following equation [17,18]:

$$\Delta_{\mathrm{trs}}H_{\mathrm{m}} = \frac{\left[Q - n\int_{T_{\mathrm{i}}}^{T_{\mathrm{trs}}} C_{p,\mathrm{m}(1)}\mathrm{d}T - n\int_{T_{\mathrm{trs}}}^{T_{\mathrm{f}}} C_{p,\mathrm{m}(2)}\mathrm{d}T - \int_{T_{\mathrm{i}}}^{T_{\mathrm{f}}} H_0\mathrm{d}T\right]}{n}(\mathrm{kJ}\cdot\mathrm{mol}^{-1}) \quad (1)$$

Table 3 Thermodynamic properties of two phase transitions obtained from three series of repeated heat–capacity measurements of 1-dodecylamine hydrochloride

Thermodynamic properties	Series 1 (x_i)	Series 2 (x_i)	Series 3 (x_i)	Mean value ($\overline{x} \pm \sigma_a$)[a]
$T_{\mathrm{trs},1}$ (K)	331.47	330.88	329.98	330.78 ± 0.43
$T_{\mathrm{trs},2}$ (K)	344.86	345.02	345.40	345.09 ± 0.16
$\Delta_{\mathrm{trs}}H_{\mathrm{m},1}$ ($\mathrm{kJ}\cdot\mathrm{mol}^{-1}$)	25.838	25.562	25.755	25.718 ± 0.082
$\Delta_{\mathrm{trs}}H_{\mathrm{m},2}$ ($\mathrm{kJ}\cdot\mathrm{mol}^{-1}$)	4.973	5.156	5.019	5.049 ± 0.055
$\Delta_{\mathrm{trs}}S_{\mathrm{m},1}$ ($\mathrm{J}\cdot\mathrm{mol}^{-1}\cdot\mathrm{K}^{-1}$)	77.950	77.255	78.051	77.752 ± 0.250
$\Delta_{\mathrm{trs}}S_{\mathrm{m},2}$ ($\mathrm{J}\cdot\mathrm{mol}^{-1}\cdot\mathrm{K}^{-1}$)	14.420	14.944	14.531	14.632 ± 0.159

$T_{\mathrm{trs},1}$ (K), $T_{\mathrm{trs},2}$ (K), $\Delta_{\mathrm{trs}}H_{\mathrm{m},1}$ ($\mathrm{kJ}\cdot\mathrm{mol}^{-1}$), $\Delta_{\mathrm{trs}}H_{\mathrm{m},2}$ ($\mathrm{kJ}\cdot\mathrm{mol}^{-1}$), $\Delta_{\mathrm{trs}}S_{\mathrm{m},1}$ ($\mathrm{J}\cdot\mathrm{mol}^{-1}\cdot\mathrm{K}^{-1}$), and $\Delta_{\mathrm{trs}}S_{\mathrm{m},2}$($\mathrm{J}\cdot\mathrm{mol}^{-1}\cdot\mathrm{K}^{-1}$) are the peak temperatures, molar enthalpies, and molar entropies of the first and second phase transitions, respectively

[a] $\sigma_a = \sqrt{\frac{\sum_{i=1}^{n}(x_i-\overline{x})^2}{n(n-1)}}$, in which n is experimental number (n = 3); x_i, experimental value of each series of repeated measurement; and $\overline{x}$, mean value

and the molar entropies $\Delta_{\rm trs}S_{\rm m}(\mathrm{J}\cdot\mathrm{K}^{-1}\cdot\mathrm{mol}^{-1})$ of the two phase transitions were calculated by

$$\Delta_{\rm trs}S_{\rm m} = \Delta_{\rm trs}H_{\rm m}/T_{\rm trs}(\mathrm{J}\cdot\mathrm{mol}^{-1}\cdot\mathrm{K}^{-1}) \tag{2}$$

where $T_{\rm i}$ in Eq. 1 was a temperature slightly lower than the starting phase transition temperature, $T_{\rm f}$ was a temperature slightly higher than the ending transition temperature, $C_{p,{\rm m}(1)}$ was the heat capacity at temperature $T_{\rm i}$, $C_{p,{\rm m}(2)}$ was the heat capacity at temperature $T_{\rm f}$, Q/J was the total heat quantity introduced to the calorimeter from temperature $T_{\rm i}$ to $T_{\rm f}$, $T_{\rm trs}$ was the transition temperature of the measured sample, n was the number of moles of the sample, and $H_0/(\mathrm{J}\cdot\mathrm{K}^{-1})$ was the heat capacity of the empty sample cell. Values of Q and H_0 were calculated with the program stored in the computer linked with the adiabatic calorimetric system, and printed along with experimental results of heat capacities.

3.4 Smoothed Heat Capacities and Thermodynamic Functions of the Compound

The smoothed molar heat capacities and thermodynamic functions were calculated based on the fitted polynomial equation of the heat capacities as a function of the reduced temperature (X) according to the following thermodynamic relations:

$$(H_T - H_{298.15}) = \int_{298.15}^{T} C_{p,{\rm m}}{\rm d}T \tag{3}$$

$$(S_T - S_{298.15}) = \int_{298.15}^{T} C_{p,{\rm m}}T^{-1}{\rm d}T \tag{4}$$

The polynomial fitted values of the molar heat capacities and fundamental thermodynamic functions of the sample relative to the standard reference temperature 298.15 K are tabulated in Table 4 at an interval of 5 K.

3.5 Results of DSC Analysis of the Compound

It can be seen from the DSC curve (Fig. 8) that there were three endothermic processes in the temperature range from 323 K to 503 K. Because the first and second peaks appearing on the DSC curve were joined together, their thermodynamic properties may be calculated by reducing down to one big peak. The onset points, peak temperatures, and molar enthalpies of the endothermic peaks were determined to be 329.13 K, 335.08 K, and 30.12 $\mathrm{kJ}\cdot\mathrm{mol}^{-1}$ for the first and second peaks, and 451.28 K, 456.66 K, and 7.83 $\mathrm{kJ}\cdot\mathrm{mol}^{-1}$ for the third peak, as shown in Fig. 8. The sum of molar enthalpies of the two phase transitions based on the heat–capacity measurements is 30.767 $\mathrm{kJ}\cdot\mathrm{mol}^{-1}$ and agrees with the value of 30.12 $\mathrm{kJ}\cdot\mathrm{mol}^{-1}$ obtained from DSC. Accordingly, the first big endothermic peak measured by DSC was in accordance with

Table 4 Smoothed heat capacities and thermodynamic functions of $C_{12}H_{25}NH_3Cl(s)$

T (K)	$C_{p,\mathrm{m}}$ ($\mathrm{J \cdot mol^{-1} \cdot K^{-1}}$)	$H_T - H_{298.15K}$ ($\mathrm{kJ \cdot mol^{-1}}$)	$S_T - S_{298.15K}$ ($\mathrm{J \cdot mol^{-1} \cdot K^{-1}}$)
80	131.20	−53.163	−290.41
85	137.41	−52.492	−282.28
90	143.51	−51.789	−274.25
95	149.48	−51.057	−266.33
100	155.33	−50.295	−258.51
105	161.07	−49.504	−250.79
110	166.69	−48.684	−243.16
115	172.20	−47.837	−235.62
120	177.60	−46.962	−228.18
125	182.89	−46.061	−220.82
130	188.07	−45.134	−213.54
135	193.16	−44.181	−206.35
140	198.16	−43.202	−199.24
145	203.06	−42.199	−192.20
150	207.88	−41.172	−185.24
155	212.63	−40.121	−178.35
160	217.31	−39.046	−171.53
165	221.92	−37.948	−164.77
170	226.48	−36.827	−158.08
175	231.00	−35.683	−151.46
180	235.47	−34.517	−144.89
185	239.92	−33.328	−138.38
190	244.35	−32.118	−131.92
195	248.78	−30.885	−125.52
200	253.21	−29.630	−119.16
205	257.65	−28.353	−112.86
210	262.12	−27.053	−106.59
215	266.62	−25.731	−100.37
220	271.18	−24.387	−94.186
225	275.80	−23.019	−88.038
230	280.50	−21.629	−81.922
235	285.30	−20.214	−75.835
240	290.20	−18.776	−69.774
245	295.22	−17.312	−63.736
250	300.38	−15.823	−57.718
255	305.70	−14.308	−51.716
260	311.18	−12.766	−45.726
265	316.86	−11.196	−39.744
270	322.74	−9.5970	−33.767

Table 4 continued

T (K)	$C_{p,\mathrm{m}}$ ($\mathrm{J \cdot mol^{-1} \cdot K^{-1}}$)	$H_T - H_{298.15K}$ ($\mathrm{kJ \cdot mol^{-1}}$)	$S_T - S_{298.15K}$ ($\mathrm{J \cdot mol^{-1} \cdot K^{-1}}$)
275	328.85	−7.9682	−27.790
280	335.19	−6.3082	−21.810
285	341.80	−4.6158	−15.822
290	348.69	−2.8897	−9.8208
295	355.89	−1.1284	−3.8026
298.15	360.58	0	0
300	363.40	0.66967	2.2379
305	371.26	2.5062	8.3055
310	379.49	4.3829	14.406
315	388.10	6.3016	20.544
320	397.12	8.2645	26.725
325	406.57	10.274	32.957
330	Phase transition		
335	Phase transition		
340	Phase transition		
345	Phase transition		
350	Phase transition		
355	500.46	38.020	116.41
360	500.99	40.524	123.41
365	501.60	43.030	130.32
367	501.85	44.033	133.07
370	502.25	45.540	137.15
375	502.91	48.053	143.90
380	503.57	50.569	150.56
385	504.23	53.088	157.15
390	504.89	55.611	163.66
395	505.56	58.137	170.10

the two phase transitions appearing on the $C_{p,\mathrm{m}}$–T curve. Meanwhile, the last endothermic peak appearing on the DSC curve corresponded to the melting process since the melting point of the compound was measured to be about 454.65 K to 456.15 K by using the microscopic melting-point device.

4 Conclusions

Low-temperature heat capacities of the title compound were measured by a newly improved adiabatic calorimeter over the temperature range from 78 K to 397 K. Two solid-to-solid phase transitions were found on the $C_{p,\mathrm{m}}$–T curve, and the phase transition mechanism was discussed. The molar enthalpies $\Delta_{\mathrm{trs}} H_{\mathrm{m}}(\mathrm{kJ \cdot mol^{-1}})$ and molar

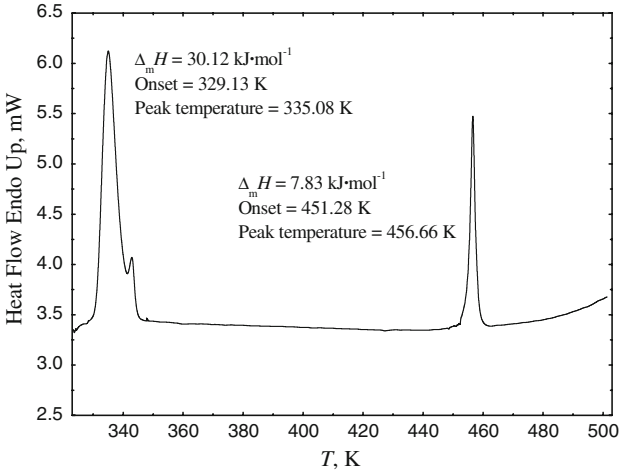

Fig. 8 DSC curve of 1-dodecylamine hydrochloride ($C_{12}H_{25}NH_3Cl$)(s)

entropies $\Delta_{trs}S_m(J \cdot mol^{-1} \cdot K^{-1})$ of the two solid-to-solid phase changes were calculated according to thermodynamic equations. Also, the relevant thermodynamic functions were determined based on the fitted polynomial equations.

Acknowledgments This study was financially supported by the National Science Foundations of China under contract NSFC Nos. 20673050 and 20973089.

References

1. W.-P. Li, D.-S. Zhang, T.-P. Zhang, T.-Z. Wang, D.-S. Ruan, D.-Q. Xing, H.-B. Li, Thermochim. Acta **326**, 183 (1999)
2. V. Busico, C. Carfagna, V. Salerno, Sol. Energy **24**, 575 (1980)
3. D.-S. Ruan, W.-P. Li, Q.-Z. Hu, J. Therm. Anal. **45**, 235 (1995)
4. K.-W. Lee, C.-E. Lee, J. Kim, J.-K. Kang, Solid State Commun. **124**, 185 (2002)
5. Z.-C. Tan, Y.-Y. Di, Prog. Chem. **18**, 1234 (2006)
6. B.E. Lang, J. Boerio-Goates, B.F. Woodfield, J. Chem. Thermodyn. **38**, 1655 (2006)
7. K. Kobashi, T. Kyomen, M. Oguni, J. Phys. Chem. Solids **59**, 667 (1998)
8. M. Sorai, K. Kaji, Y. Kaneko, J. Chem. Thermodyn. **24**, 167 (1992)
9. T. Matsuo, H. Suga, Thermochim. Acta **88**, 149 (1985)
10. A. Inaba, J. Chem. Thermodyn. **15**, 1137 (1983)
11. D.A. Ditmars, S. Ishira, S.S. Chang, G. Bernstein, E.D. West, J. Res. Natl Bur. Stand. **87**, 159 (1982)
12. X.-K. Gao, J.-M. Dou, D.-C. Li, F.-Y. Dong, D.-Q. Wang, J. Mol. Struct. **733**, 181 (2005)
13. Y.-Y. Di, J.-T. Chen, Z.-C. Tan, Thermochim. Acta **471**, 70 (2008)
14. W.-W. Yang, Y.-Y. Di, Z.-F. Yin, Y.-X. Kong, Z.-C. Tan, Int. J. Thermophys. **30**, 542 (2009)
15. D.G. Archer, J. Phys. Chem. Ref. Data **22**, 1441 (1993)
16. R. Kind, S. Plesko, H. Arend, R. Blinc, B. Zeks, J. Seliger, B. Lozar, J. Slak, A. Levstik, C. Filipic, V. Zagar, G. Lahajnar, F. Milia, G. Chapuis, J. Chem. Phys. **71**, 2118 (1979)
17. Z.-C. Tan, L.-X. Sun, S.-H. Meng, L. Li, F. Xu, P. Yu, B.-P. Liu, J.-B. Zhang, J. Chem. Thermodyn. **34**, 1417 (2002)
18. Y.-Y. Di, Z.-C. Tan, X.-M. Wu, S.-H. Meng, S.-S. Qu, Thermochim. Acta **356**, 143 (2000)